Plasma chemistry and diagnostic in an ArN2H2 microwave expanding plasma used for nitriding treatments

Said Touimi, Jean-Louis Jauberteau, Isabelle Jauberteau, Jacques Aubreton

Plasma chemistry and diagnostic in an Ar-N_2-H_2 microwave expanding plasma used for nitriding treatments.

S. Touimi, J. L. Jauberteau,[a)] I. Jauberteau, J. Aubreton

SPCTS-UMR 6638 CNRS, Faculté des Sciences, 123 av A. Thomas, 87060 Limoges, France.

[a)] Electronic mail for correspondence: jean-louis.jauberteau@unilim.fr

Abstract

This paper reports on mass spectrometry analysis performed downstream a microwave discharge in Ar-N_2-H_2 gas mixture in nitriding conditions. Investigations are focused on the main simple radicals NH_2, NH and N, and on the molecular species NH_3 and N_2H_2 produced. Because of wall desorptions due to catalytic effects, we must develop a specific method taking into account both wall desorption and dissociative ionization effects, in order to correct the mass spectrometer signal intensity. The relative concentrations of the previous species are studied in various gas mixtures. Correlations are made between the plasma chemistry and plasma parameters (electron density and energy electron distribution function), measured by means of Langmuir probes spatially resolved within the plasma expansion. These results show the efficiency of ternary gas mixtures (Ar-N_2-H_2) to produce electrons and N_xH_y species used in plasma nitriding process.

1. introduction.

Microwave discharge sustained in Ar-N_2-H_2 gas mixtures are used in a wide range of industrial applications. Like ammonia synthesis /1/, nitriding processes for surface treatment of metallic or polymer pieces /2,3,4/ and for the elaboration of optical or electronic devices /5/. The efficiency of such plasma processes depends on the knowledge of the various elementary mechanisms involved in the gas phase and at the surface of the reactor wall or of the work pieces. In previous papers /6, 7/, we have shown that the surface oxide reduction of thin molybdenum films, in the nitriding treatment, depends on the gas composition in the plasma expansion and on the distance between the work piece surface and the discharge centre. We confirm correlations between nitrided layers characteristics, discharge expansion

conditions, gas composition and Langmuir probe measurements performed within the plasma expansion.

The purpose of this paper is to investigate the various chemical species produced within the discharge and in the expansion in nitriding treatment conditions. We make correlation between the gas compositions and the plasma parameters in the working conditions. Investigations are performed by means of mass spectrometer downstream a microwave discharge and by means of spatially resolved Langmuir probe in the plasma expansion in nitriding conditions

2. Experimental set-up.

The experimental setup is shown on Figure 1. It consists of a microwave discharge (SAIREM generator working at 2.45 GHz) produced in a quartz tube (internal diameter 16mm and external diameter 19mm). In order to keep a constant wall temperature, the quartz tube is refreshed by means of air cooling. A Roots pumps (70-700 m^3/hour) with an adjustable rotational speed is used and a gas flow velocity ranges from 10 to 30 m/s is maintained constant in the stainless tube (inner diameter 50mm) located above the discharge and collecting species produced within the plasma. The flow is considered as a “plug” flow and the velocity has been previously measured by means of absorption spectroscopy measurements on $Ar(^3P_2)$ metastable species produced in an Ar microwave discharge. The total pressure in the discharge tube is held constant and ranges from 10 to 100 Pa. The mass spectrometer (QMG 421 Balzers) is fixed above this stainless steel tube at 30cm from the discharge. The ionization of neutral species is performed using the electron impact technique by means of a cross beam source. Before each experiment, the reactor is heated and pumped at 10^{-4} Pa and maintained at this pressure for several hours by means of a molecular pump in order to clean the reactor wall. Because the quadrupole cannot operate at pressure lower than 10^{-3} Pa, a specific two-stage differential pumping device has been made and is detailed in ref /8/. It consists of two independent coaxial chambers fitted into each other and equipped with separated Turbo pumps units. The quadrupole is located at the middle of the inner chamber (see Figure1). A charged particles collector (Langmuir probe) is located in the grounded stainless steel tube. Results show that no ion or electron is crossing this area located 20cm below the mass spectrometer sample hole. Thus, investigations are performed in a region without charged particle and no reaction between charged particles and neutral species occurs in this tube between the discharge and the mass spectrometer. The present study gives

information of reactivity between neutral species only. Even though, in the microwave expanding plasma used for molybdenum nitriding process, reactive processes between charged particles and neutral species are efficient probably until the substrate holder /7/.

3. Mass spectrometry analysis downstream the discharge.

In discharges sustained in the ternary gas mixture Ar-N_2-H_2, NH_x species partly results of plasma catalysis processes on the reactor wall /9, 10/ or are directly produced in the discharge bulk. A large part of the mass spectrometer signal intensity is due to desorbed species from the reactor wall. This effect occurs when the discharge is off or on. So, it is necessary to take into account this trouble in order to measure the real effect of the discharge on the gas composition.

3.1. The main species detected

The main species detected in the Ar-N_2- H_2 discharge afterglow are observed at m/q=1, 2, 14, 15, 16, 17, 18, 28, 30 32 and 40 and correspond to H^+, H_2^+, N^+, NH^+, NH_2^+, NH_3^+ (or OH^+), H_2O^+(residual water), N_2^+, $N_2H_2^+$, O_2^+(residual oxygen) and Ar^+ respectively. $N_2H_4^+$ and NH_4^+ are probably not produced in these experiments. No significant change on the peak intensity is observed at m/q=32 and 18 when the discharge off is switched on. Because of the low stability of NH_4 species and of its short lifetime in the ground state with respect to the dissociation process (0.43 ns) /11, 12/, NH_4 concentration downstream the discharge is insignificant. In a previous paper /13/, NH_4^+ has been observed by means of mass spectrometer within a N_2-H_2 discharge. In this case, this stable ion is probably directly produced in the discharge and not in the ionization chamber of the mass spectrometer by direct ionization of the neutral form (NH_4). The particular case of N_2H_4, will be discussed later in this text.

For all species (i) detected, the signal intensity measured downstream the discharge, where ion concentration is negligible, is the sum of two contributions. One is due to the direct ionization of species (i) and the second is due to the dissociative ionization of larger species (j). This effect can be written /8/,

$$I_i = I(i^+/i) + \sum_j I(i^+/j) = T_i.\sigma_{(i+/i)}(\varepsilon_e).n_i + T_i.\sum_j (\sigma_{(i+/j)}(\varepsilon_e).n_j) \quad (1)$$

Where, $\sigma_{(i+/i)}(\varepsilon_e)$ is the ionization cross section due to the direct ionization of i species and $\sigma_{(i+/j)}(\varepsilon_e)$ is the dissociative ionization cross section of j species producing i ions. T_i is the transmission factor. It depends on m/q, on the pressure and on the electron energy in the ionization chamber. When the measurements are performed within the discharge, we must add a term to the signal given by Equation 1, which is due to ions (i) produced within the discharge.

The main problem is now to separate in the total signal intensity the part due to the direct ionization of i species from the part due to the dissociative ionization processes of j species larger than i species. In the next part, we will investigate these different contributions in the case of the different species detected.

3.1.1. The case of NH_3.

This species is detected at m/q=17 and consequently, the signal measured can be mixed with that of OH^+ ion, which is due to the dissociative ionization process of H_2O (residual water) in the ionization chamber. The contribution of each dissociation process can be estimated, considering the change of the signal intensity versus the electron energy used in the ionization chamber. This method was previously reported by Toyoda et al /14-15/ in the case of CH_2 and CH_3 radicals produced in a methane containing discharge. Figure 2 shows the change of the signal intensity measured for m/q=17 versus the electron energy. Results are compared to the signal intensity calculated assuming the direct ionization process using cross section values given by Märk et al /16/, Tarnovsky et al /17/ and Rejoub et al /18/ in the case of hydrogenated and deuterated molecules. Results are also compared to the signal intensity calculated assuming the dissociative ionization process of H_2O producing OH^+ and using the cross section values measured by Straub et al /19/ in the case of deuterated molecules (OD^+/D_2O). Before any comparison, the measured signal intensity obtained for m/q=17 is corrected, taking into account the change of the emission current intensity versus the electron energy in the ionization chamber. This effect is due to the angular divergence of the electron beam at the entrance slit of the ionization chamber. The correction method has been detailed in previous works /8/ and correction factor has been measured using the signal intensity corresponding to Ar(m/q=40). In Figure 2, the signal intensity is calculated in reference to the value obtained at 25 eV using the fit polynomial through the experimental values. It can be seen that the signal intensity calculated in the case of the direct ionization and using the cross

section values given by Märk et al /16/ is larger than the signal intensity calculated using the cross section values given by Tarnovsky et al /17/ or Rejoub et al /18/. This change could be explain by the fact that both authors Tarnovsky and Rejoub use deuterated ammonia, and consequently are not disturbed by the signal due to OH^+(m/q=17) ion, which is due to the dissociative ionization of residual water in the reactor. In the present experiments, the signal intensity value measured ranges between the value calculated assuming only the direct ionization of NH_3 and the value calculated in the case of the dissociative ionization of H_2O. The signal intensity measured for m/q=17 is the sum of the two contributions, one is due to the direct ionization of ammonia and the other to the dissociative ionization of water. This can be written,

$$I_{(m/q=17)} = I(NH_3^+/NH_3) + I(OH^+/H_2O) = T_{(m/q=17)}[(\sigma(NH_3^+/NH_3)\, n_{NH3}) + (\sigma(OH^+/H_2O) n_{H2O})]$$

Where, T(m/q=17) is the transmission factor of the mass spectrometer at m/q=17, $\sigma(NH_3^+/NH_3)$ and $\sigma(OH^+/H_2O)$ are the ionization cross section for the direct ionization of ammonia and for the dissociative ionization of water respectively. n_{NH3} and n_{H2O} are the concentration of ammonia and water respectively.
Assuming only the direct ionization of the water, the signal intensity measured for m/q=18 is given by,

$$I_{(m/q=18)} = T_{(m/q=18)}\, \sigma(H_2O^+/H_2O) n_{H2O}$$

Where $T_{(m/q=18)}$ is the transmission factor for m/q=18, $\sigma(H_2O^+/H_2O)$ is the ionization cross section for the direct ionization of the water and n_{H2O} is the residual water concentration.
Mixing these two last equations, the contribution to the signal intensity due to the direct ionization of ammonia is given by,

$$I(NH_3^+/NH_3) = I_{(m/q=17)} - [T_{(m/q=17)}/T_{(m/q=18)}\, \sigma(OH^+/H_2O)/\sigma(H_2O^+/H_2O)\, I_{(m/q=18)})] \quad (2)$$

In this equation, the ratio $T_{(m/q=17)}/T_{(m/q=18)}$ is calculated using results reported in ref (8). Consequently, the part due to the direct ionization of NH_3, can be calculated by means of the signal intensity measured at m/q=17 and m/q=18 and using Equation 2. Results are reported on Figure 2. It can be seen a good agreement between results of Equation 2 and the previous ones calculated considering the direct ionization cross section values given in the literature in

the case of deuterated species (Tarnovsky or Rejoub /17-18/). The part due to the direct ionization of NH_3 ranges from 70 to 90% of the total signal intensity measured for m/q=17, when electron energy ranges from 25 to 70 eV. The part of the signal results mainly of the dissociative ionization of water and can be easily suppressed considering the difference between the signal measured when the discharge is on and off. This simple way for the signal correction will be used in the next part of the article in order to suppress the contribution due to the wall desorption in the afterglow.

3.1.2. The case of NH_x radicals.

The same considerations have been performed in the case of the simple radicals NH_2^+, NH^+ and N^+ detected in the discharge afterglow.

Figure 3 displays the signal intensity of NH_2 taking into account the change of the emission current intensity versus the electron energy. The results are compared to the values calculated assuming only the direct ionization of NH_2 and using the ionization cross-section values given by Tarnovsky et al /17/. They are also compared to the calculated values obtained assuming the dissociative ionization process of ammonia and using the ionization cross section values given by Tarnovsky /17/ and Märk et al /16/. Results obtained using these two references are quite different. In one case (Tarnovsky), we can consider that there is no contribution due to the dissociative ionization of ammonia. In the second case (Märk), this contribution would be quite obvious. Assuming that this last case gives an overestimation of the dissociative ionization effect, we will consider it in the following part of this paper, to correct the signal of NH_2. In these conditions (using Märk et al cross section values), results show that the part of the direct ionization of NH_2 is larger than 70% of the total signal, when electron energy ranges from 25 to 70eV.

As previously done for NH_3 and NH_2, Figures 4 and 5 give results obtained in the case of NH and N. Experimental values are compared versus the electron energy to the signal intensity calculated assuming only the direct ionization of the two radicals. We use the cross section values measured by Tarnovsky et al /17/ for NH and Brook et al /20/ for N. It can be seen a good agreement between experimental and calculated values for both species. This shows that the signal measured for m/q=14 and 15 result mainly of the direct ionization of NH and N.

3.1.3. The case of N_2H_2 (diimide)

Figure 6 displays the signal intensity measured for m/q=30 versus the electron energy. As previously, intensities values are corrected taking into account the change due to the emission current in the ionization chamber. Comparison is performed with calculated values assuming only the dissociative ionization of Hydrazine (N_2H_4), and using ionization cross section values given by Syage et al /21/. A good agreement is observed between the two curves. This show that the signal intensity measured for $N_2H_2^+$ could be ascribed to the dissociative ionization of hydrazine. However, $N_2H_4^+$ ion is not detected in these experiments and is expected to be easily detected at these electron energies when N_2H_4 is produced /22/. Although, the signal intensity measured for $N_2H_2^+$ is the same that the value calculated assuming only the dissociative ionization of hydrazine, the previous remarks show that N_2H_4 is not significantly produced in the present experiments and the signal measured for m/q=30 is probably mainly due to the direct ionization of N_2H_2. Comparison of experimental values to calculations assuming only the direct ionization of N_2H_2, is necessary in order to confirm the previous conclusion. However, no data about this ionization process is available in the literature. According to Stothard et al /23/, the main channel reaction of NH_2 +NH_2 at low pressure and ambient temperature is producing N_2H_2 and H_2. The reaction rate constant is rather significant $k=1.3.10^{-12}$ cm^3 s^{-1}. But, the energy difference between NH_2+NH_2 and N_2H_4, is too large and a three body channel reaction must be considered in order to produce N_2H_4 and to dissipate the energy excess. The third body could be no reactive species in the gas volume ($k=7.0.10^{-14}$ cm^3s^{-1} in He at 1mbar) or at low pressure it is more probably the wall reactor. Considering a Ni(100) surface at temperature ranges from 200 to 450K, Huang et al /24/ have shown that the primary mechanism for diimide formation is the recombination of an adsorbed NH surface intermediate.

This first study shows that in the case of NH and N the signal measured by mass spectrometry is mainly due to the direct ionization of the neutral radical. However, in the case of NH_2 and NH_3, it results of two contributions: The direct ionization and the dissociative ionization of larger species. These contributions depend on the electron energy in the ionization chamber. The figure 7 displays the part due to the direct ionization of NH_3 and NH_2 compared to the total signal intensity measured for m/q=16 and 17, versus electron energy, and considering the cross section values given by Märk et al /16/ for NH_2 (case of an overestimation). For both species, the dissociative ionization contributes to less than 30% to the total signal for electron energy lower than 70 eV.

3.2. The correction of the mass spectrometry signal.

Before any analysis by means of mass spectrometer in nitriding conditions, it is necessary to correct the signal intensity measured for each species, removing the part due to the dissociative ionization of larger species. As previously shown on Figures 2, 3, 4 and 5, this part remains lower than 30%, in our experimental conditions. In the case of NH and N, this correction can be neglected. In the case of NH_3, the dissociative ionization is mainly due to desorbed water from the wall, which can be easily withdrawn considering the difference between the signal intensity measured with and without discharge. In case of NH_2, the part due to the dissociative ionization is mainly due to NH_3 and the correction factor depends on the electron energy and is displays on Figure7. In the case of N_2H_2, correction is not possible because ionization cross section values are not available.

In a previous work /10/, we report a more accurate method taking into account the different dissociative processes contributing to the signal intensity measured for each species. Polynomial equations are calculated using the relative concentrations values, NH_2/NH_3, NH/NH_3 and N/NH_3. The coefficients of these polynomial equations depend on the cross sections values of the different ionization processes involved. This should be a more accurate method that the previous one. However, because of the strong uncertainty on the cross section values reported in the literature, 15% for the parent ionization cross section values and 18% for the dissociative ionization cross section values/17/, the different coefficient of the polynomial equations are determined with a too large uncertainty (typically from 30% to 60%, according to the coefficient). The error on relative density is very large and can be over 100% according to the experimental conditions, especially in gas composition with high N_2% and H_2%, producing a large amount of NH_3. For these reasons in the present works corresponding to experiments performed in nitriding conditions, this method cannot be used because of the too large error and the previous one is preferable.

3.3. Mass spectrometer diagnostics in nitriding conditions.

In previous works, it was shown that a (Ar-25%N_2-30%H_2) plasma exposure at 8cm from the centre of the discharge seems the most efficient ternary gas mixture to reduce the oxide layers remaining at the surface of a molybdenum film /7/. Correlations had already been performed with electron density and plasma propagation conditions. As previously related this gas composition lead to a better plasma expansion due to a larger electron density than in pure nitrogen or in other ternary gas mixture with lower H_2 contents /7,8/. The present work gives

complementary results about the chemical gas composition in such ternary gas mixture used in expanding microwave plasma.

Two gas mixtures have been investigated to carry out this study. They are:

The gas mixture 1:

It contains (0 to 30%) H_2 injected in the binary mixture (64%Ar-36%N_2). It corresponds to a gas flow containing 180 sccm Ar, 100 sccm N_2.

The gas mixture 2:

It contains (0 to 15%) H_2 injected in the binary mixture (91%Ar-9%N_2). It corresponds to a mixture with 1000 sccm Ar and 100 sccm N_2.

In the different series N_2 gas flow is equal to 100 sccm and the total pressure Ar+N_2 is kept constant and is equal to 100 Pa. The pressure is controlled by changing the rotational speed of the Roots blower pumps. The second gas mixture contains more Argon than the first one, and recombination processes of NH_x radicals are expected to be less important than in the first one because of the dilution. For the two gas mixture, the microwave power used for the chemical analysis is 150 W.

3.3.1. The case of NH_x species.

Analysis, corresponding to different nitriding conditions, are performed downstream the discharge. Figure 8 and 9 displays the relative signal intensity measured by means of mass spectrometer, N/NH_3, NH/NH_3 and NH_2/NH_3, versus %H_2 injected in Ar+N_2 binary mixture, considering the two previous gas mixtures respectively. In these figures the main radical produced is NH_2 then NH and N. The ratio NH_x/NH_3 slowly decreases with increasing % H_2. In the first gas mixture, the ratio NH_2/NH_3 ranges from 0.1 to 0.5 all over the %H_2 under investigation. The ratio NH/NH_3 and N/NH_3 ranges roughly from 0.1 to 0.01 and lower than 0.01 for the first ratio and the second respectively. In the gas mixture2, the relative NH_2 concentration produced is larger than in the gas mixture 1, and is over 1. The two other ratios N/NH_3 and NH/NH_3 are almost identical to those obtained in the former gas mixture. This increase in the relative NH_2 concentration can be explained by the larger Ar flow rate used in the mixture 2. Radicals produced in such conditions are more diluted and the recombination process is decreasing. The effect of the dilution is more evident on NH_2 that on the two other radicals which concentrations are one or two magnitude orders lower.

Figure 10, shows the relative concentration of ammonia compared to the argon (NH_3/Ar), versus the %H_2 mixed to Ar+N_2, in the two gas mixtures (64%Ar-36%N_2) and (91%Ar-

9%N_2). It can be seen that for the two binary gas mixtures under investigation, the relative concentration of NH_3 remains nearly the same and roughly linearly depends on H_2% injected. No saturation is observed on the figure. Comparison with results displayed on Figure 8 and 9 prove that the concentration of radicals NH_2, NH and N also increase with % H_2 increasing in both Ar-N_2 binary mixtures. On Figure 10 are also reported three ternary gas mixtures which will be discussed later in the text.

Two different reaction channels are involved to produce N_xH_y species in an Ar-N_2-H_2 discharge. They are plasma catalysis processes (heterogeneous reactions) /9/ or volume reactions (homogeneous reactions) /25/. In the present experiments, the concentration of NH_2>(NH or N). In a previous work /10/, we have shown that NH>NH_2 at low % N_2 injected (98.7%Ar-1.3%N_2). For larger N_2%, NH concentration is similar to NH_2 concentration or even lower in N_2-H_2 gas mixture. This agrees with the present experiments. However, Helden et al /25/ obtained in N_2-H_2 a NH concentration larger than NH_2 and they show that the NH concentration decreases and NH_2 concentration increases with %N_2 decreasing. This is in contradiction with our results. Such different behaviour can be understood considering a change in the dominant reactive mechanism involved. In the present experiments, the inner reactor diameter is 50mm and the pressure is 100Pa, whereas in the case of Helden et al /25/, the plasma is expanding supersonically in the reactor, which inner diameter is 400mm and the pressure is 20KPa in the cascaded arc plasma source and 20 Pa to 100 Pa in the reactor. Because of the low pressure and of the low reactor diameter, the dominant reaction channels are probably heterogeneous reaction in our experiments, whereas homogeneous mechanisms are dominant in the case of Helden et al /25/, where NH and NH_2 are mainly produced by the reactions,

$N+H_2 \rightarrow NH + H$ ($k=4.10^{-16}$ m^3s^{-1})

$NH_3 + H \rightarrow NH_2 + H_2$ (($k=4.10^{-18}$ m^3s^{-1} at 1750K).

Because of the large activation energy needs for the last reaction, radical concentrations are NH>NH_2 in the bulk plasma, where homogenous reaction dominate. However, the reaction rate can be enhanced by means of fast H atom injected within the plasma /25/. Similar processes with fast ions have been related in the case of ion-molecule reaction /26/.

It is worth noting that in this reactive scheme, NH_3 is supposed produced by catalytic plasma reaction /9/ and reacts with the species produced in the plasma expansion because of the recirculation flow produced within the reactor.
In the case where the surface reaction dominates, NH produced within the discharge, reacts on the reactor wall (stainless steel) according to /9, 10/,

$NH_s + H \rightarrow NH_{2s}$

As previously, NH_3 results of the surface reactions,

$NH_{2s} + H \rightarrow NH_3$
And
$NH_s + H_2 \rightarrow NH_3$.

Where, NH_s is adsorbed NH species.
As previously related, at low $\%N_2$ injected, $NH > NH_2$. This behaviour as been observed on Ni(100) surface by Huang et al /24/ and it can be explained by the large adsorption of H_2 on the wall, which stabilise NH and stop the surface reaction of NH_s with H_s, producing NH_2.

3.3.2. The case of N_2H_2:

Figure 11 shows the relative concentration ratio (N_2H_2/NH_3) versus % H_2 injected in the two previous binary mixtures $Ar+N_2$. It can be seen that the relative density of N_2H_2 produced remains the same in both mixtures and that a maximum is observed at about 5% H_2.
According to Huang et al /24/, the primary mechanism for diimide formation is the recombination of an adsorbed NH surface intermediate. This mechanism can be written,
$NH_s + NH_s \rightarrow N_2H_2$.
The admixture of H_2 in the gas composition increases the coadsorbed hydrogen density (on a Ni(100) surface), and stabilizes the NH intermediate, increasing the surface concentration of imide in the hydrogen-deficient surface environment in the 200K-450K /24/. Consequently the diimide concentration is significantly increased in the presence of post-adsorbed hydrogen even in a 10^{-7} Torr hydrogen flow /24/. For larger $\%H_2$ injected in the gas mixture, the surface sites are saturated with hydrogen and the recombination surface mechanism of NH_s producing N_2H_2 is now decreasing. Thus, there is a maximum of efficiency to produce N_2H_2 by means of

the previous surface reaction. In our results, this maximum is observed at about 5% H_2 injected.

3.4. Correlation between plasma chemistry and plasma parameters.

In order to make correlations between the plasma parameters in the expanding plasma and the gas composition, investigations have been performed by means of Langmuir probe downstream the discharge in the reactor previously used for plasma nitriding treatment /7, 8/. The Langmuir probe is fixed in the expanding plasma along the expansion axis and can be moved according to this axis from the tube discharge exit to the substrate holder. This experimental set-up is detailed in ref 7 and 8. The electron energy distribution function has been measured using the Druyvesteyn equation and the numerical simulation of harmonic component method previously reported /27/. Measurements have been performed at injected powers equal to 400 W and 200 W and in three gas mixtures, corresponding to Ar-30%N_2-12%H_2, Ar-8%N_2-10%H_2, Ar-25%N_2-30%H_2. As previously reported /7/, a ternary mixture containing Ar-N_2-H_2 can be used to produce plasma expansion below the discharge tube exit in the reactor even with a large amount of H_2 and N_2 (more than 50%) mixed in Ar. Whereas in a binary mixture containing Ar-N_2 or Ar-H_2, the plasma expansion is strongly shrinking in the discharge tube for H_2 or N_2 concentration larger than (1% for H_2 and 5% for N_2). Figure 12 shows the electron density measured at 400W, versus the distance in the plasma expansion. Measurements have been performed in the three previous mixtures, Ar-30%N_2-12%H_2, Ar-8%N_2-10%H_2 and Ar-25%N_2-30%H_2, in the binary mixtures, Ar-1%N_2, Ar-50%N_2 and in pure Ar. The electron density is calculated using the electron current value measured at the plasma potential /27/. Binary mixtures containing Ar-H_2 are strongly disturbed even at a low %H_2 injected (<1%) and accurate results are not available. As expected the electron density decreases with increasing distance from the tube discharge exit. It can be seen that when N_2 is injected in argon, the electron density decreases with the % N_2 increasing, the same effect could be observed with H_2. This behaviour can be ascribed to the increase of inelastic collisions in the gas mixture. Surprisingly, in the ternary gas mixtures Ar-25%N_2-30%H_2 and Ar-8%N_2-10%H_2, the electron density increases compared to results obtained in pure argon discharge even for a (N_2+H_2) admixture larger than 50%. Nevertheless in the case of Ar-30%N_2-12%H_2, the electron density remains very low, lower than in Ar-50%N_2.

Figure 13 displays the electron distribution function measured at 200 W, 3cm below the discharge exit in the three ternary gas mixtures under investigation (Ar-30%N_2-12%H_2, Ar-

8%N_2-10%H_2 and Ar-25%N_2-30%H_2). It can be seen that for Ar-30%N_2-12%H_2, the electron distribution function is smaller than those obtained for the two other gas mixtures and in Ar-8%N_2-10%H_2, the electron distribution function is the largest. As expected, these results agree with the previous ones displayed on Figure 12, the electron density can also be calculated using the electron distribution functions /27/. These results prove the good efficiency of the second and third gas mixtures for the plasma expansion even at 200W, and the difficulty encountered with the first one to sustain the plasma expansion at a power lower than 400W.

Comparison with previous results obtained by means of mass spectrometer in the same gas mixtures (see the Figure 8, 9, 10), show that the two first gas mixtures correspond to plasma containing low density of NH_x radicals and NH_3 molecules. Whereas the third gas mixture corresponds to plasma containing a large amount of NH_x radicals and NH_3 molecules. In the particular case of the second gas mixture, N_2 and H_2 and NH_x species are largely diluted in Ar, compared to the two other ones. These remarks show that the plasma expansion in the reactor is efficient in plasma containing N_2 or H_2 strongly diluted in Ar or in plasma containing a large concentration of N_2 and H_2 (more than 50%) and producing a large amount of ammonia and radicals NH_x. This behaviour can be explained looking at the ionization threshold values of the different species observed in these plasmas. The ionization threshold values of Ar, N_2 and H_2 are 15.75, 15.58 and 15.426 eV respectively /28/. The ionization threshold of NH_3 is 10.166 eV, that of NH_2 is 11.22 eV and NH is 12.8 eV /28/. Moreover the ionization cross section values of NH_x species are larger than ionization cross section values of N_2 and H_2 /16, 17, 18, 28/. Consequently, NH_x radicals or NH_3, increases the efficiency of ionization processes within the plasma, and therefore increase the electron density. Consequently, the plasma expansion is easier in gas mixture containing large amounts of NH_x species. H. Nigai et al /29/, have observed that the admixture of a little amount of N_2 in H_2, drastically increases the electron density, since the total ionization cross section of N_2 is larger than that of H_2 and the dissociation of H_2 is enhanced to generate more H radicals, which contribute to the etching of organic low k film. In our experiments, the electron density increases with NH_x concentration increasing. This could also contributes to increase NH_x dissociation processes and to enhance oxide reduction at the surface layer, as it was previously related /7-8/.

4. Conclusion.

Investigations have been performed downstream a microwave discharge sustained in Ar-N_2-H_2 gas mixtures, by means of mass spectrometry. In a first time we develop a method in order to correct the measured signal disturbed by wall desorption and dissociative ionization processes. In a second part we study the relative concentration of the main radicals and molecules produced in various gas compositions previously used for thin molybdenum layers nitriding treatment. Then we make correlations between the plasma chemistry and the plasma parameters measured by means of Langmuir probe spatially resolved in the plasma expansion. Results show that with ternary mixtures (Ar-N_2-H_2) a large amount of N_2+H_2 can be mixed in the discharge (up to 50%), even at low power (200W) without plasma shrinking. In binary gas mixture plasma expansion cannot be obtained at such power for concentration larger than 5% for N_2 or 3% for H_2 mixed to Ar. This behaviour can be explained by the large amount of NH_x radicals, and NH_3 produced. Due to the low ionization threshold values of these species compared to those of N_2, H_2 and Ar, the production of these species gives rise to an increase of ionization process number and of the electron density. Consequently, the plasma expansion in the reactor is improved. Moreover, the electron density increase gives rise to an increase of dissociation processes, producing NH_x radicals. As it has been already reported, in the case of H atoms, these radicals could act on the substrate layers, reducing oxide /7, 8/.

Acknowledgements: This work has been supported by La Région Limousin.

References

[1] Uyama. H, Matsumoto. O 1989 plasma Chemistry and plasma process 9 13-24 or Uyama. H, Nakamura. T, Tanaka. S, Matsumoto. O 1993 plasma chem. And plasma process 13 117-131

[2] Schram. D. C 2002 Pure.Appl.Chem74 369-380

[3] Jauberteau. I, Jauberteau. J. L, Cahoreau. M, Aubreton. J 2001 Trends in vacuum Science and Technology 4 78-99 Editor Menon. J Resarch Trends, Trivandrum, India

[4] Leroy. C, Czerwiec. T, Gabet. C, Belmonte. T 2001 Surface and Coating Technology 142-144 241-247

[5] Kobayashi. N, 1998 Journal of Crystal Growth 195 228-233

[6] Jauberteau. I, Jauberteau.J.L, Aubreton.J, 2002 J. Phys. D : Appl. Phys 35 665

[7] Jauberteau. I, Jauberteau.J.L, Goudeau. P, Soulestin. B, Marteau. M, Cahoreau. M, Aubreton.J 2009 Surface and Coating Technology 203 1127-1132

[8] Jauberteau. J. L, Jauberteau. I, Aubreton.J, 2007 International Journal of Mass Spectrometry 15-24

[9] Gordiets. B, Ferreira. C. M, Pinheiro. M. J, Ricard. A, 1998 Plasma source Sci. Technol 7 379-388

[10] Jauberteau. J. L, Jauberteau. I, Aubreton. J, 2002 J. Phys. D : Appl. Phys 35 665-674

[11] Williams. B. W, Porter. R. F 1980 J. Chem. Phys 73 5548-5604

[12] Smith. J. M, Chupka. W. A 1996 Chem. Phys. Letters 250 589-596

[13] Fujii. T, Iwase. K, Selvin. P. C 2002 International Journal of Mass spectrometry 216 169-175

[14] Kojima. H, Toyoda. H, Sugai. H 1989 Appl. Phys. Letters 55 13 1292-1294

[15] Toyoda. H, Kojima. H, Sugai. H 1989 Appl. Phys . Letters 54 16 1507-1509

[16] Märk. T. D, Egger. F, Cheret. M 1977 J. Chem. Phys 115 5053-5058

[17] Tarnovsky. V, Deutsch. H, Becker. K 1997 International Journal of Mass spectrometry 167/168 69-78

[18] Rejoub. R, Lindsay. B. G, Stebbings. R. F 2001 J. Chem. Phys 115 5053-5058

[19] Straub. H. C, Lindsay. B. G, Smith. K. A, Stebbings. R. F 1998 J. Chem. Phys 108 109-116

[20] Brook. E, Harrison. M. F. A, Smith. A. C. H 1978 J. Phys. B: Atom. Molec. Phys 11 3115-3132

[21] Syage. J. A 1992 J. Chem. Phys 97 6085-6107

[22] Foner. S. N, Hudson. R. L, 1978 J. Chem. Phys 68 3162-3168

[23] Stothard. N, Humpfer. R, Grotheer H. H 1995 Chem. Phys. Letters 240 474-480

[24] Huang. S. X, Rufael. S. T, Gland. J. L 1993 Surface sciences Letters 290 L673-676

[25] van Helden J. M, van Den Oever. P. J, Kessels. W. M. M, van de sanden. M. C. M, Schram. D. C, Engeln. R, 2007 J. Phys. Chem. A 111 11460-11472

[26] Weber. M. E, Armentrout. P. B 1989 J. Chem. Phys 90 2213-

[27] Jauberteau. J. L, Jauberteau. I 2008 Plasma Source. Sci Technol 17 015019

[28]*National Institue of Standards and Technology (NIST),* http://physics.nist.gov/PhysRefData/Ionization.html

[29] Nagai. H, Takashima. S, Hiramatsu. M, Hori. M, Goto. T 2002 J. Appl. Phys 91 2615-2621

Figure captions.

Figure 1. Experimental set-up.

Figure 2. Mass spectrometer signal intensity measured for NH_3^+ (m/q=17) versus electron energy in the ionization chamber. Comparison with the signal intensity calculated using cross section values given in the literature in the cases of the direct ionization of NH_3 (Märk, Tarnovsky, Rejoub) and of the dissociative ionization of water producing OH^+ (m/q=17) (Straub).

Figure 3. Mass spectrometer signal intensity measured for NH_2^+ (m/q=16) versus electron energy in the ionization chamber. Comparison with the signal intensity calculated using cross section values given in the literature in the cases of the direct ionization of NH_2 (Tarnovsky) and of the dissociative ionization of NH_3 (Märk, Tarnovsky).

Figure 4. Mass spectrometer signal intensity measured for NH^+ (m/q=15) versus electron energy in the ionization chamber. Comparison with the signal intensity calculated assuming the direct ionization of NH using cross section values given in the literature (Tarnovsky).

Figure 5. Mass spectrometer signal intensity measured for N^+ (m/q=14) versus electron energy in the ionization chamber. Comparison with the signal intensity calculated assuming the direct ionization of N using cross section values given in the literature (Brook).

Figure 6. Mass spectrometer signal intensity measured for $N_2H_2^+$ (m/q=30) versus electron energy in the ionization chamber. Comparison with the signal intensity calculated assuming the dissociative ionization of hydrazine, using cross section values given in the literature (Syage).

Figure 7. Contribution to the total signal intensity measured at m/q=17 and 16 of the direct ionization of NH_3 and NH_2, versus electron energy.

Figure 8. The relative signal intensity measured by means of mass spectrometer N/NH_3, NH/NH_3 and NH_2/NH_3, versus $\%H_2$ injected in $Ar+N_2$ binary mixture, in the case of the first gas mixture.

Figure 9. The relative signal intensity measured by means of mass spectrometer N/NH_3, NH/NH_3 and NH_2/NH_3, versus $\%H_2$ injected in $Ar+N_2$ binary mixture, in the case of the second gas mixture.

Figure 10. The relative concentration of ammonia compared to the argon (NH_3/Ar), versus $\%H_2$ mixed to $Ar+N_2$, in the two gas mixtures (64%Ar-36%N_2) (circle) and (91%Ar-9%N_2) (square). The ternary mixtures pointed on the graph bring back to comments displayed in section 3.4.

Figure 11. The relative concentration ratio (N_2H_2/NH_3) versus % H_2 injected in the binary mixtures (64%Ar-36%N_2) (full circles) and (91%Ar-9%N_2) (empty squares).

Figure 12. The electron density measured by means of a langmuir probe versus distance from the tube discharge exit. Measurements are performed at 400W, in different gas mixtures.

Figure 13. The electron energy distribution function measured by means of a langmuir probe and numerical simulation of harmonic components method, in the case of the three ternary gas mixtures under investigation.

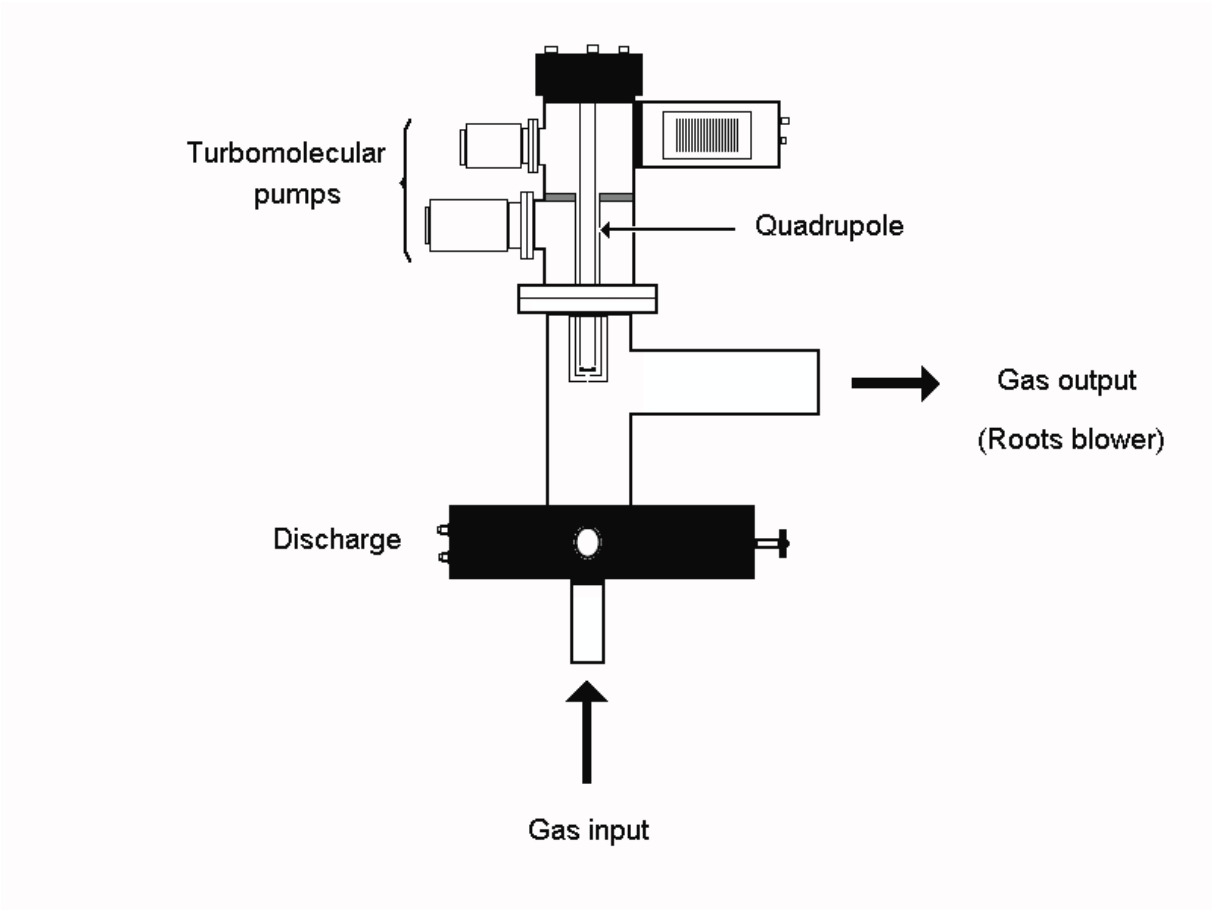
Turbomolecular
pumps
Quadrupole
Gas output
(Roots blower)
Discharge
Gas input

FIG.1.

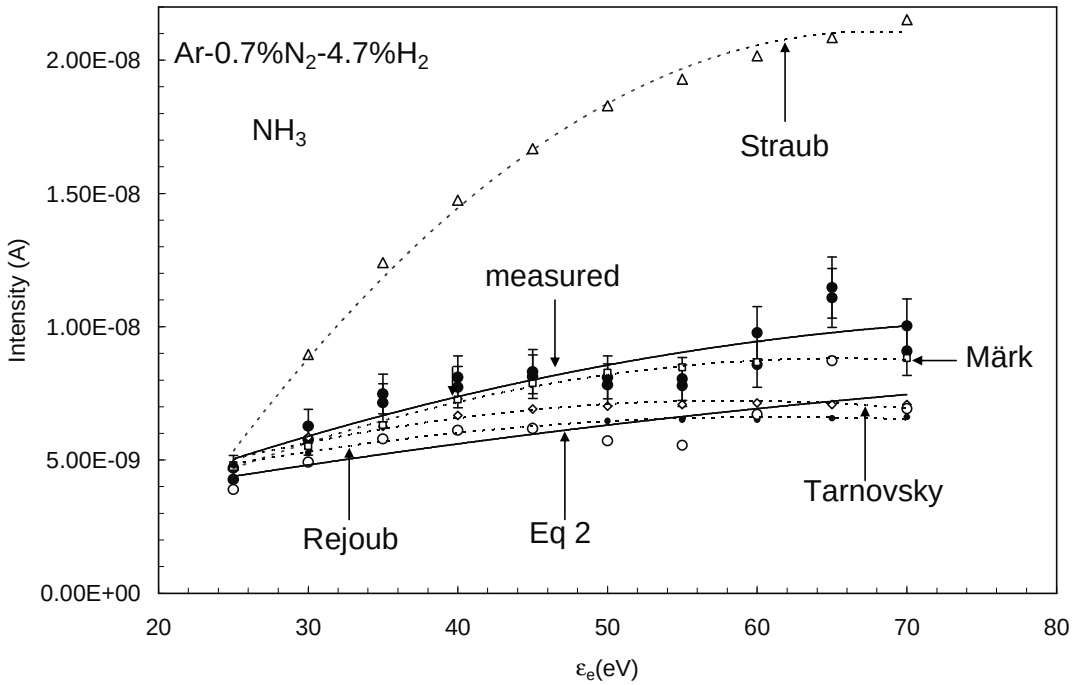
Ar-0.7%N2-4.7%H2
NH3
Straub
measured
Märk
Tarnovsky
Rejoub
Eq 2
Intensity (A)
2.00E-08
1.50E-08
1.00E-08
5.00E-09
0.00E+00
20
30
40
50
60
70
80
εe(eV)

FIG.2.

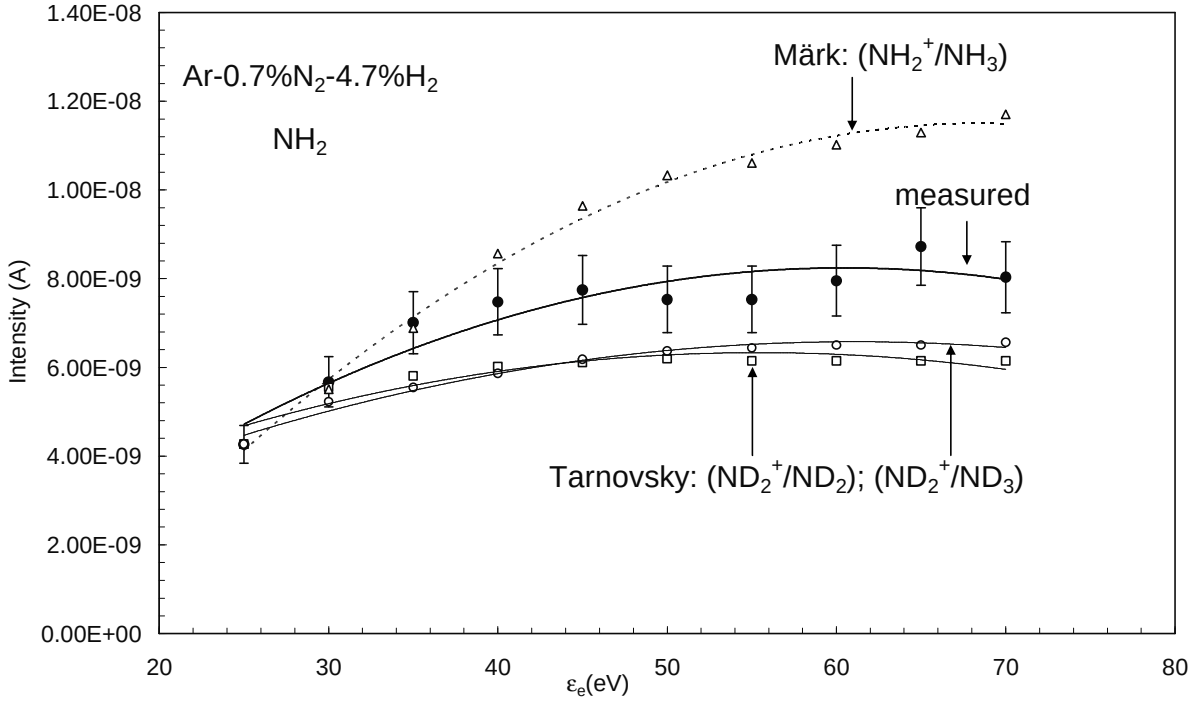
1.40E-08
1.20E-08
1.00E-08
8.00E-09
6.00E-09
4.00E-09
2.00E-09
0.00E+00
Intensity (A)
20
30
40
50
60
70
80
εe(eV)
Ar-0.7%N2-4.7%H2
NH2
Märk: (NH2+/NH3)
measured
Tarnovsky: (ND2+/ND2); (ND2+/ND3)

FIG.3.

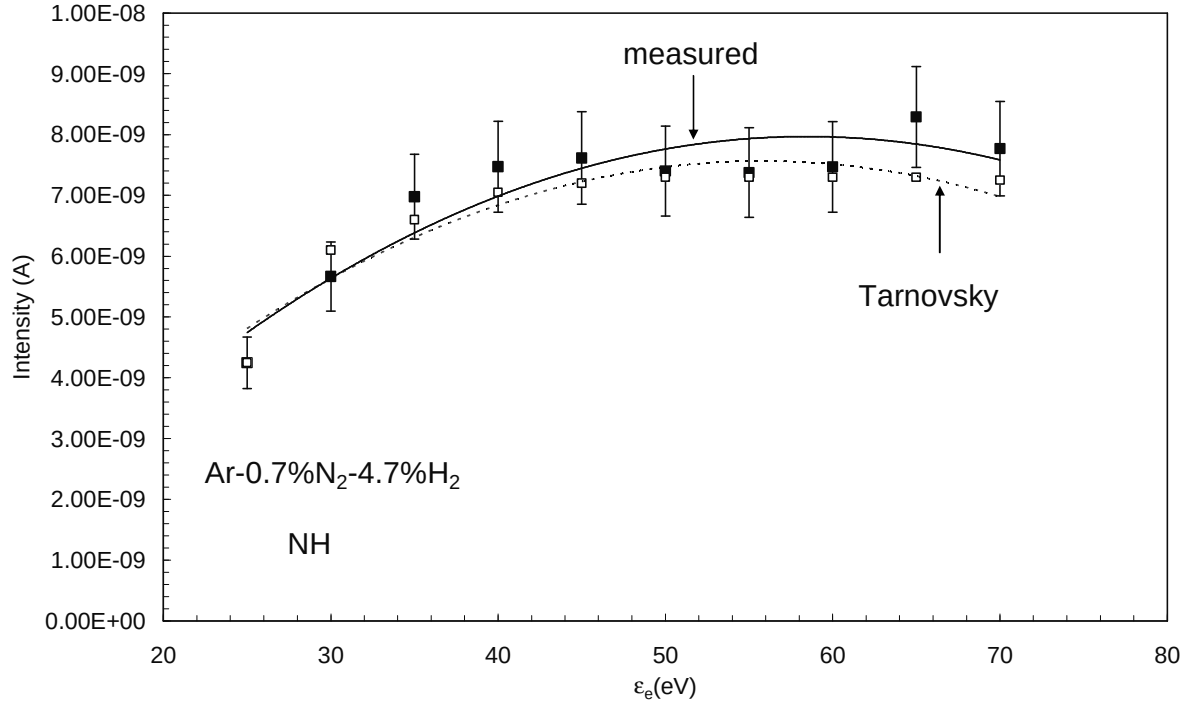
1.00E-08
9.00E-09
8.00E-09
7.00E-09
6.00E-09
5.00E-09
4.00E-09
3.00E-09
2.00E-09
1.00E-09
0.00E+00
Intensity (A)
20
30
40
50
60
70
80
εe(eV)
measured
Tarnovsky
Ar-0.7%N2-4.7%H2
NH

FIG.4.

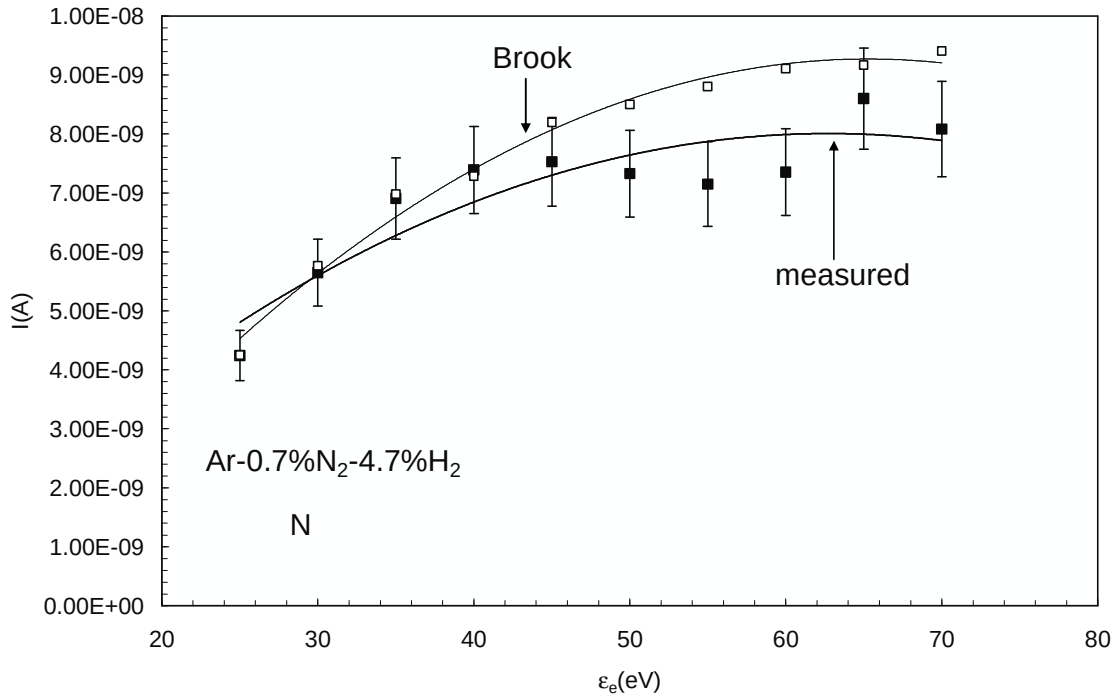
1.00E-08
9.00E-09
8.00E-09
7.00E-09
6.00E-09
5.00E-09
4.00E-09
3.00E-09
2.00E-09
1.00E-09
0.00E+00
I(A)
Brook
measured
Ar-0.7%N2-4.7%H2
N
20
30
40
50
60
70
80
εe(eV)

FIG.5.

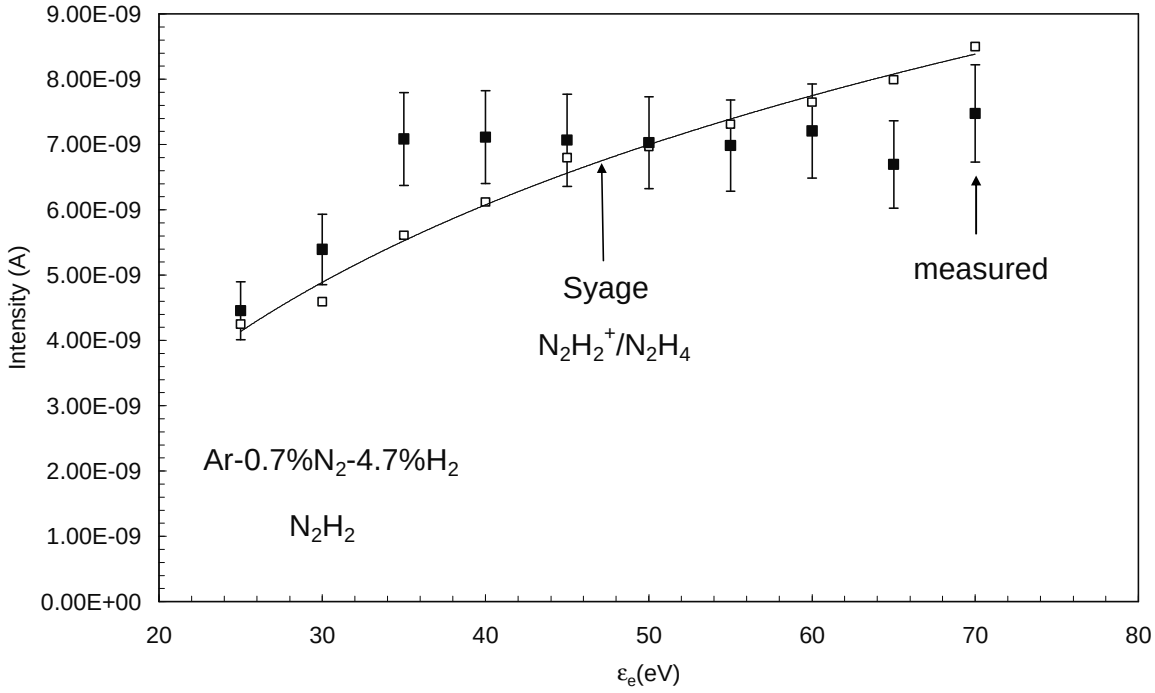
9.00E-09
8.00E-09
7.00E-09
6.00E-09
5.00E-09
4.00E-09
3.00E-09
2.00E-09
1.00E-09
0.00E+00
Intensity (A)
Syage
N2H2+/N2H4
measured
Ar-0.7%N2-4.7%H2
N2H2
20
30
40
50
60
70
80
εe(eV)

FIG.6.

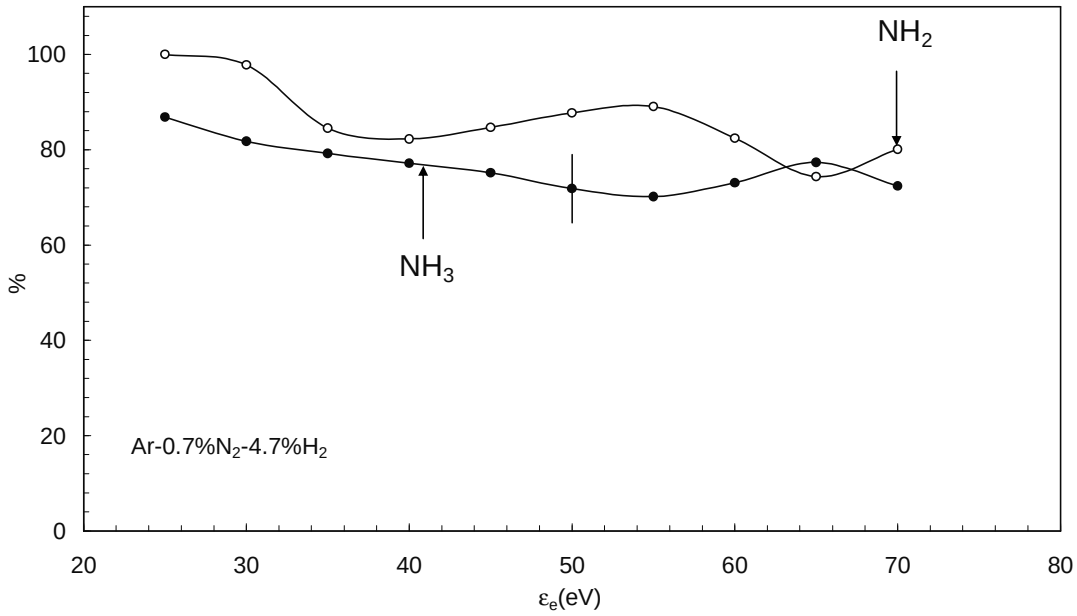
NH2
NH3
%
Ar-0.7%N2-4.7%H2
εe(eV)

FIG.7.

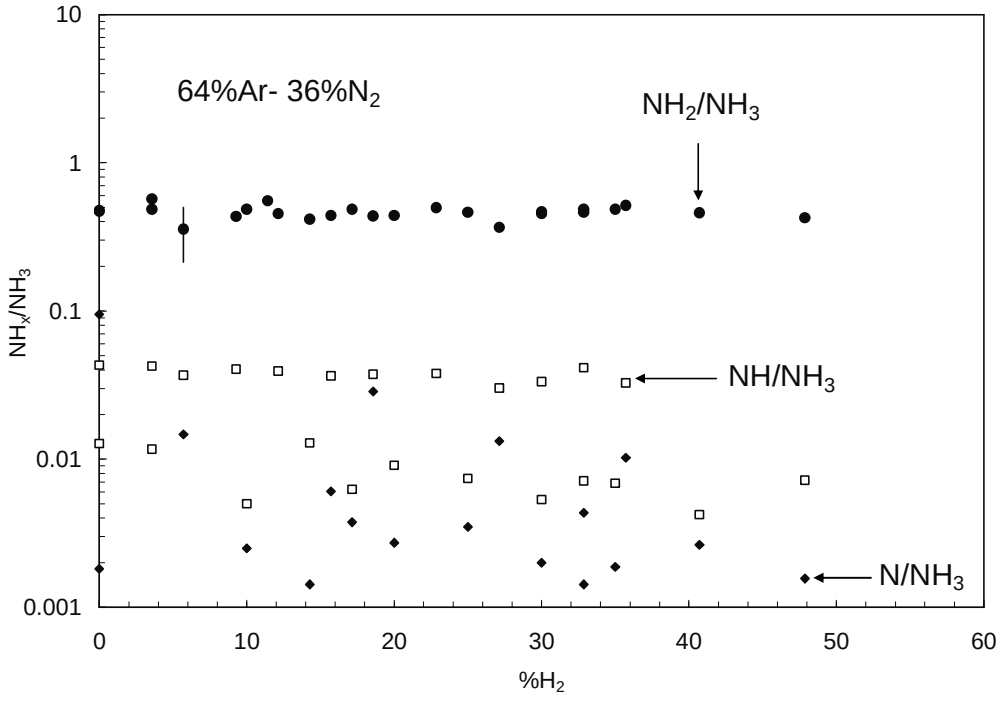
64%Ar- 36%N2
NH2/NH3
NH/NH3
N/NH3
NHx/NH3
%H2

FIG.8.

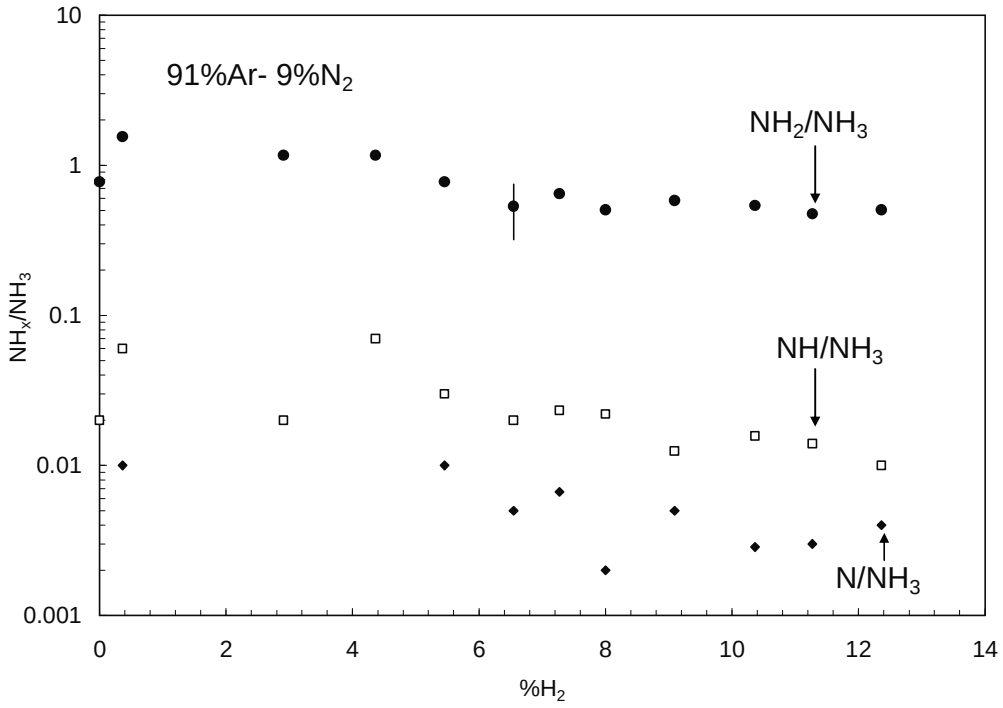
10
1
0.1
0.01
0.001
0
2
4
6
8
10
12
14
NH_x/NH_3
$\%H_2$
91%Ar- 9%N_2
NH_2/NH_3
NH/NH_3
N/NH_3

FIG.9.

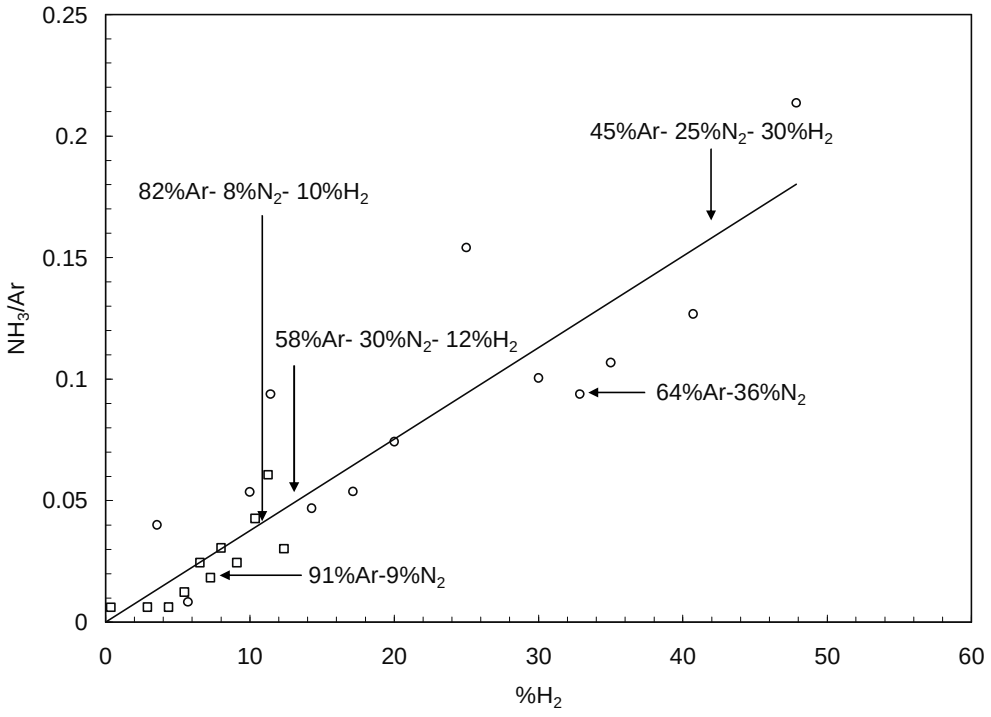
0.25
0.2
0.15
0.1
0.05
0
0
10
20
30
40
50
60
NH_3/Ar
$\%H_2$
45%Ar- 25%N_2- 30%H_2
82%Ar- 8%N_2- 10%H_2
58%Ar- 30%N_2- 12%H_2
64%Ar-36%N_2
91%Ar-9%N_2

FIG.10.

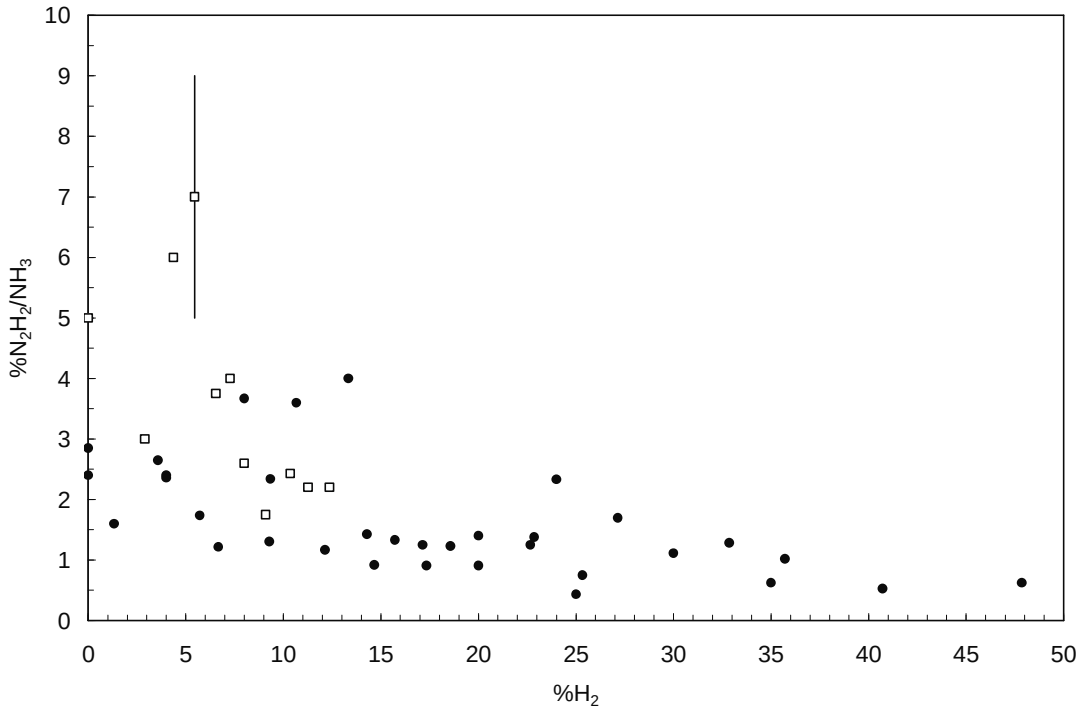
%N2H2/NH3
%H2
0
1
2
3
4
5
6
7
8
9
10
0
5
10
15
20
25
30
35
40
45
50

FIG.11.

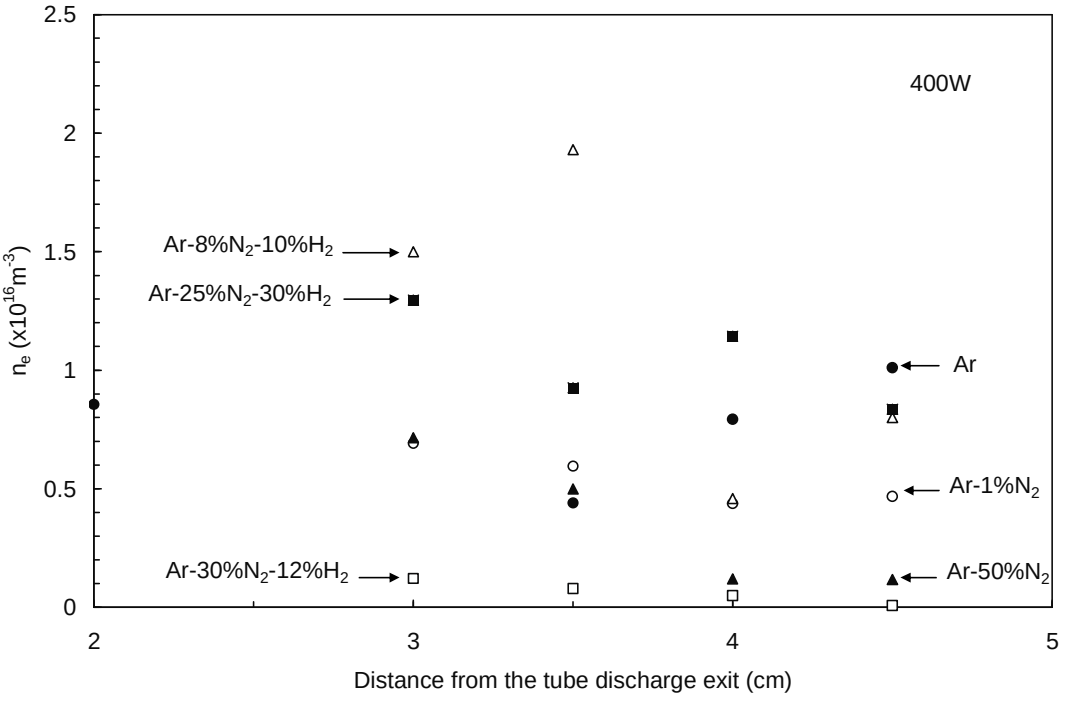
400W
Ar-8%N2-10%H2
Ar-25%N2-30%H2
Ar-30%N2-12%H2
Ar
Ar-1%N2
Ar-50%N2
ne (x10^16m^-3)
Distance from the tube discharge exit (cm)
0
0.5
1
1.5
2
2.5
2
3
4
5

FIG.12.

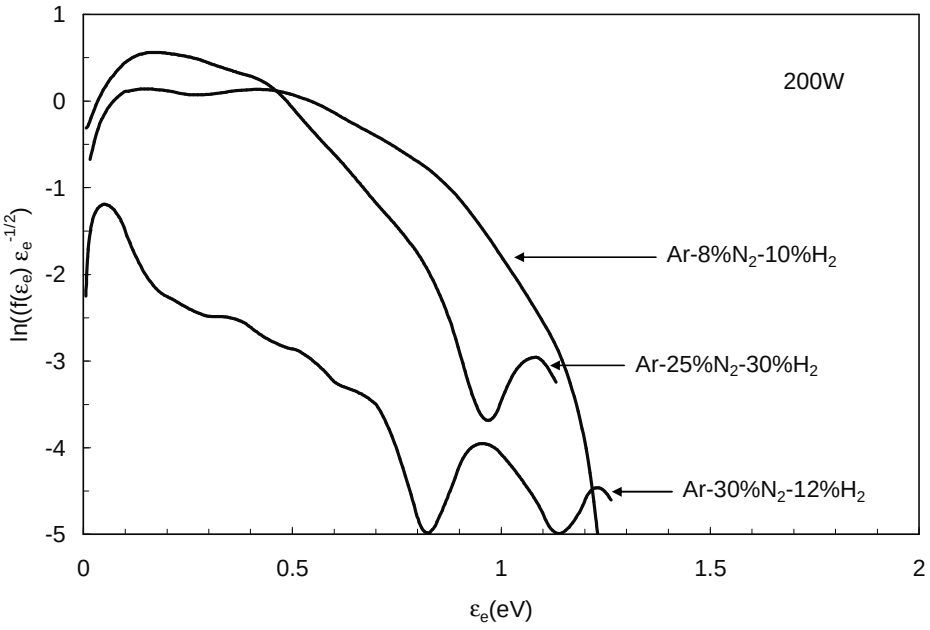
200W
Ar-8%N2-10%H2
Ar-25%N2-30%H2
Ar-30%N2-12%H2
ln((f(εe) εe-1/2)
εe(eV)
1
0
-1
-2
-3
-4
-5
0
0.5
1
1.5
2

FIG.13.